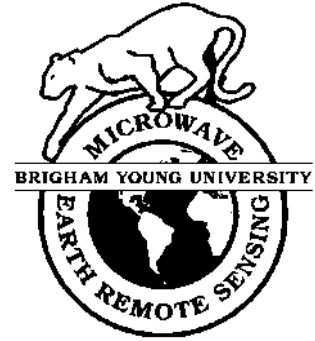


Brigham Young University
Department of Electrical and
Computer Engineering

459 Clyde Building
Provo, Utah 84602



Multipath Analysis of the QuikSCAT Calibration Ground Station

Arden Anderson

16 April 2001

MERS Technical Report # MERS 01-01
ECEN Department Report # TR-L131-01.01

**Microwave Earth Remote Sensing (MERS)
Laboratory**

© Copyright 2001, Brigham Young University. All rights reserved.

MULTIPATH ANALYSIS OF THE QUIKSCAT CALIBRATION GROUND STATION

Arden Anderson
Brigham Young University, MERS Laboratory
459 CB, Provo, UT 84602
801-378-4884, FAX: 801-378-6586, ardena@et.byu.edu

Abstract— The BYU QuikSCAT Calibration Ground Station (CGS) team has performed an analysis on the effects of multipath on the CGS. The process of analysis includes creating an electronic database of the surrounding area after careful site survey and dividing the surround into discrete surfaces. It finds the contribution of unwanted signal reflections from each of the surfaces and adds up all of the contributions.

The analysis assumes simple scattering, i.e. the signal bounces no more than once before hitting the CGS antenna. It also assumes that each patch of ground is at a constant height and has a constant radar cross-section. The surrounding buildings and features are assumed to have a constant radar cross-section. The analysis shows that the effects of multipath on the CGS are negligible.

Introduction

As an important instrument to aid in global weather monitoring, SeaWinds on QuikSCAT was successfully launched on June 19, 1999. This satellite radar sensor orbits the earth, making measurements of the radar cross section of the earth below within the swath that it covers. To ensure the instrument's accuracy and dependability, a ground station has been built at the NASA White Sands Testing Facility in White Sands, New Mexico. This ground station receives the signal of the satellite as it passes overhead and illuminates the receiving antenna of the ground station. Ground processing uses the received signal to calibrate the attitude, position and timing of the satellite.

Noise may affect the integrity and usefulness of the received signal. Some possible sources of noise are atmospheric conditions, temperature inconsistencies and multipath. Multipath occurs when portions of the satellite signal scatter off of the CGS surroundings and are indirectly received by the antenna, as shown in Figure 1. This multipath may lead to power and/or timing errors in the measurement. This report documents BYU's Calibration Ground Station multipath simulation, which provides an initial evaluation of the effects of multipath on the received signal.

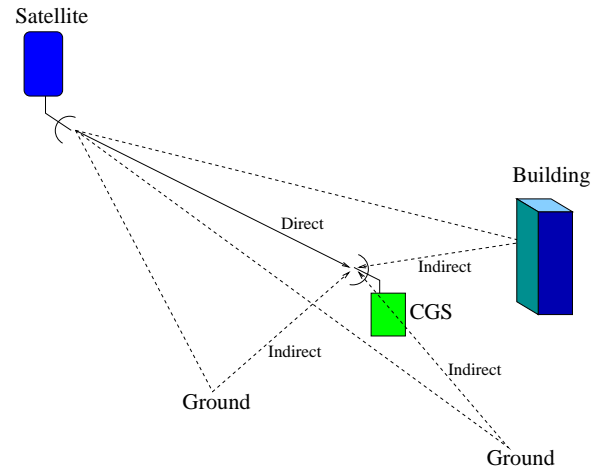


Figure 1: Visualization of multipath. The transmitted signal bounces off of the surroundings of the receiver and arrives at a later time, out of sync with the directly received signal.

Simulating multipath can be an extensive and computationally intensive task. In order to limit the complexity of this analysis, a key assumption has been made: Assume that the satellite signal bounces no more than once before reaching the receiving antenna. This effectively means that if the signal bounces more than once, its strength is small enough to neglect.

This assumption allows us to model the multipath as a collective reradiation of the transmitted signal off of the surroundings of the CGS. The surroundings of the CGS can be classified into three different groups. The first of these groups is the surrounding terrain. This includes all of the ground within sight of the CGS. As will be shown later, the further away the signal bounces off of the ground, the weaker its effect on the ground station signal. Thus, there is a cutoff distance and the ground beyond this is neglected in this analysis. The second group is the neighboring buildings. All of the buildings, walls and large objects in the vicinity of the CGS belong to this group. The third and last group is the CGS roof features. This includes the corrugated roof of the ground station, the lightning rods attached to the roof, as well as the radome cover of the antenna. This analysis considers the

multipath caused by the first two groups, the surrounding terrain and buildings. The effect of the roof features is currently under investigation in a separate analysis.

The multipath analysis is a three part process. The first part of the analysis is the discretization of the scatterers. This includes a site survey and the discretization of the terrain and buildings into individual surface patches. The second part is the geometry analysis. This considers each of the surface patches and computes important geometrical parameters. The third part is an interference strength analysis, which computes the strength of the reradiated signal from each surface patch and adds them all up to determine the total multipath interference strength and compares it to the strength of the desired, directly received signal.

Discretization of Scatterers

Recently, Peter Yoho and Arden Anderson visited the CGS at the White Sands testing facility. There, under the direction of Jim Lux from JPL, they carefully surveyed the area surrounding the CGS. They determined the location of all of the buildings and other prominent features, such as parking lots and water reservoirs, in the vicinity of the CGS.

To familiarize the reader with the surroundings of the CGS, Figure 2 shows a portion of a published map of the area. Manipulating the data collected from the site survey yields a simple electronic map of the area. After discretizing the buildings and other features into 62 individual triangular patches, the data is summarized as shown in Figure 3.

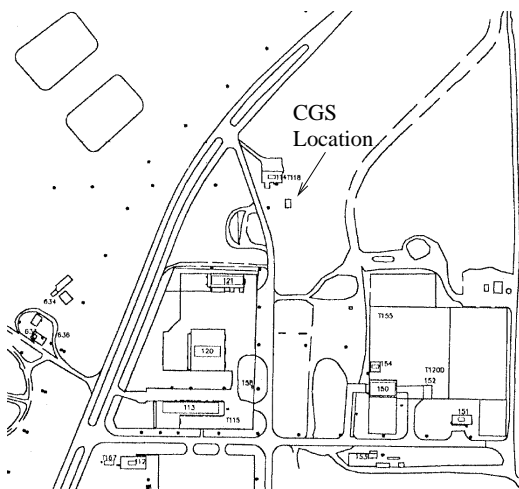


Figure 2: CGS site map

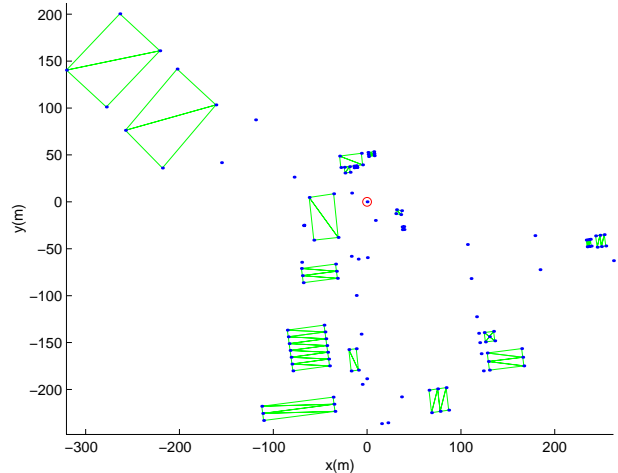


Figure 3: Electronic map of area surrounding the ground station. The surrounding buildings and features are divided into 62 separate triangular surfaces. The x, y coordinates and height of each are measured in m with respect to the CGS antenna location

The surrounding terrain is likewise divided into individual triangular patches. The triangular surfaces make up rings of constant distance from the CGS and extend out to cover all of the ground within 500 m from the CGS. For simplification purposes, we assume the terrain to be flat, at a constant elevation height of -2m with respect to the ground station. Note that later, a worst case bistatic cross section is assumed, which accounts for approximations made at this step. The resulting 464 triangles are shown in Figure 4.

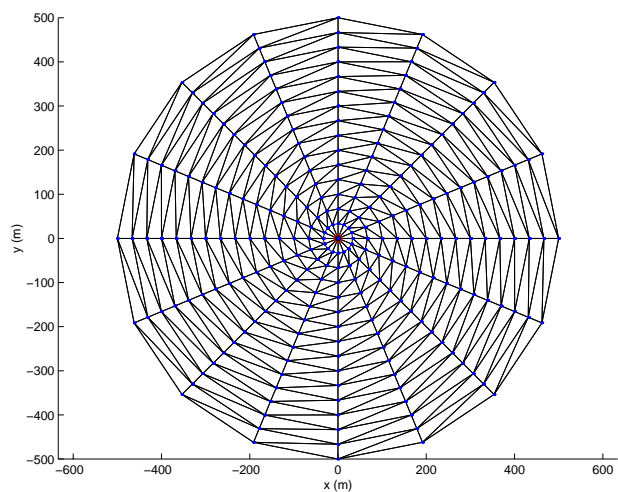


Figure 4: Surrounding Terrain divided into 464 individual Patches

Geometry Analysis

For each triangular surface, we compute the pertinent geometrical information. For a given assumed spacecraft location, the vector representing the incoming signal is v_{in} , the vector of the specular reflection is v_{spec} , the vector connecting the surface to the ground station antenna is v_{out} , and the vector normal to the surface is v_n . From these vectors, we compute θ_{out} , θ_{rec} , R_i , and A_i , where

- θ_{out} = angle between v_{spec} and v_{out}
- θ_{rec} = angle between v_{in} and v_{out}
- R_i = distance between scatterer and CGS antenna
- A_i = area of surface as seen from the satellite.

The geometry of the problem is shown in Figure 5.

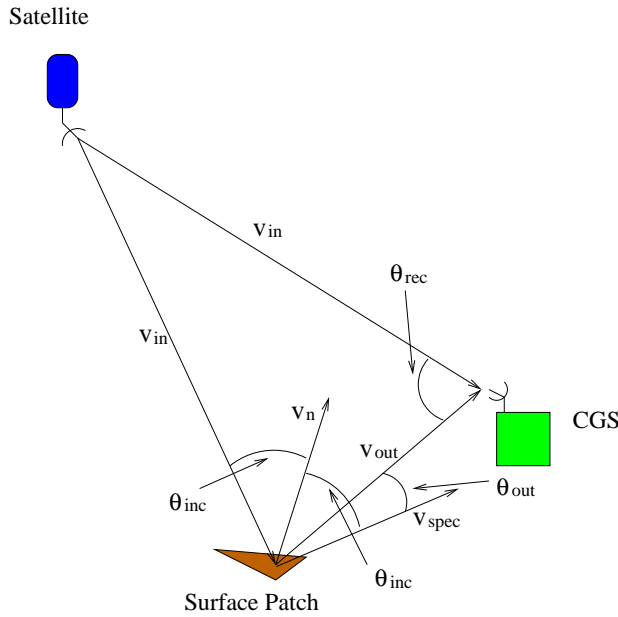


Figure 5: Geometry of an arbitrary surface patch. Because the large distance of the satellite from the CGS, the vector connecting the satellite to the CGS and that connecting the satellite to the surface patch are approximated as equal in length and direction.

The resulting geometry calculations from the buildings and the terrain are shown in Figures 6 and 7, respectively.

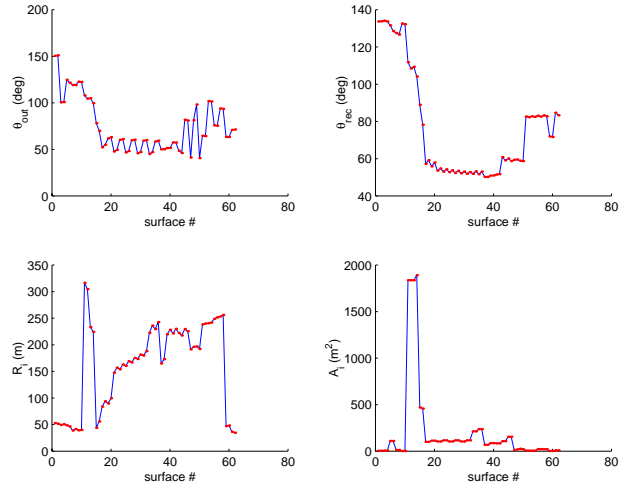


Figure 6: Geometry results for surrounding buildings. The x axis represents the patch number of the surface, which is arbitrarily assigned. For each surface, θ_{out} and θ_{rec} are never lower than 45°

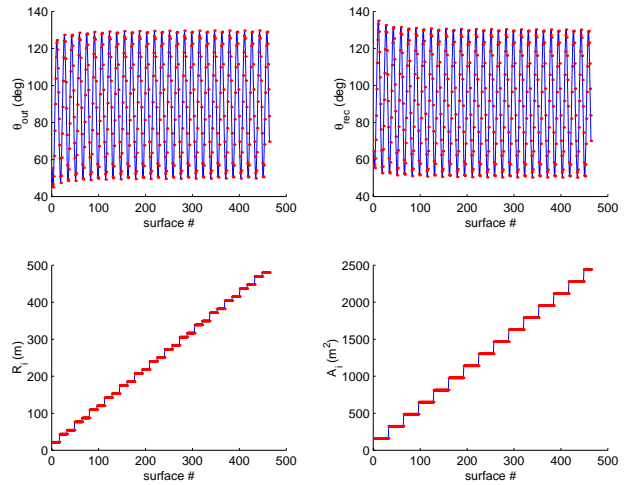


Figure 7: Geometry results for surrounding terrain. The x axis represents the patch number of the surface, which is arbitrarily assigned. The area of the patches increases as the distance from the CGS increases. θ_{out} and θ_{rec} are never lower than 45° .

Interference Strength Evaluation

The knowledge of the geometrical parameters of each surface patch allows us to calculate the power of the reradiated satellite signal received by the CGS antenna. The relationship between the transmitted power and the received power of a radar system is defined by the radar equation. One form of the bistatic radar equation sums the contribution from each possible scatterer, as given in [1] by

$$P_r = \frac{\lambda^2}{(4\pi)^3} \sum_{i=1}^N \frac{P_t G_i^2 \sigma^0 \Delta A_i}{R_i^4}. \quad (1)$$

Equation (1) assumes the transmitter and the receiver to be the same instrument. For separate transmitters and receivers, G_i^2 becomes $G_t G_i$ and R_i^4 becomes $R_t^2 R_i^2$. In this particular application, P_t , G_t and R_t are constant, allowing Equation (1) to be rewritten as

$$P_r = \frac{\lambda^2 P_t G_t}{(4\pi)^3 R_t^2} \sum_{i=1}^N \frac{G_i \sigma^0 \Delta A_i}{R_i^2}, \quad (2)$$

where

- P_r = power received
- P_t = power transmitted
- G_t = gain at transmitting antenna
- G_i = gain at receiving antenna in the direction of the scatterer
- λ = wavelength of the transmitted signal
- R_t = distance between satellite and surface patch
- R_i = distance between surface patch and CGS
- ΔA_i = area of each incremental surface patch
- σ^0 = the generalized radar cross section of the patch.

Equation (2) represents the power received at the CGS after the signal has reflected off of the surroundings, in this case the multipath, or interference. The power received at the CGS directly (i.e. the desired signal which has not bounced) is defined in [2] by Equation (3), and is also known as the link, or beacon, equation,

$$P_r = \frac{P_t G_t \lambda^2 G_r}{(4\pi)^2 R_i^2}. \quad (3)$$

where G_r is the gain at the receiving antenna in the direction of the satellite. Dividing Equation (2) by Equation (3), we obtain an interference-to-signal ratio,

$$\frac{P_{r_{indirect}}}{P_{r_{direct}}} = \frac{\sigma^0}{4\pi G_r} \sum_{i=1}^N \left(\frac{G_i \Delta A_i}{R_i^2} \right). \quad (4)$$

In this interference-to-signal ratio, A_i and R_i are computed directly by the geometry analysis. G_i is obtained by taking θ_{rec} and looking up its corresponding gain within the CGS antenna pattern. θ_{rec} is computed by the geometry analysis and slices through the CGS antenna pattern are shown in Figure 8.

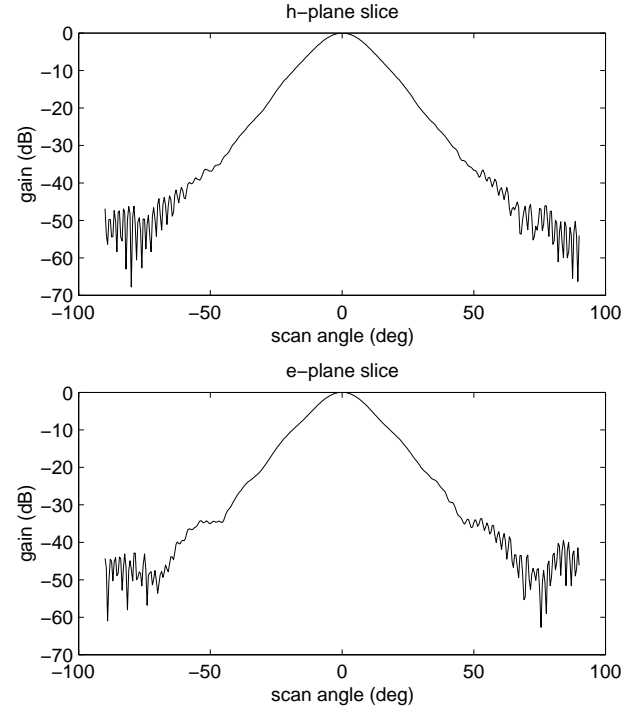


Figure 8: Perpendicular slices through the CGS antenna pattern. The main beam, as is evident in the figure, is very broad. This is according to the CGS design, to minimize the sensitivity of the gain of the received signal when the antenna points at the satellite.

Since the CGS antenna points directly at the satellite during reception, G_r is approximated as 1. σ^0 is a measure of the reflective properties of a scattering surface and is dependent on the geometry of the problem. In particular, it is dependent on the angle between the specular reflection of the transmitted signal and the vector pointing to the receiving antenna. This angle is labelled θ_{out} in this analysis and is computed in the geometry analysis. σ^0 is large if θ_{out} is small and it is small if θ_{out} is large. This dependence on θ_{out} is depicted in Figure 9 for scatterometer systems, in which the transmitting and receiving antenna are one and the same.

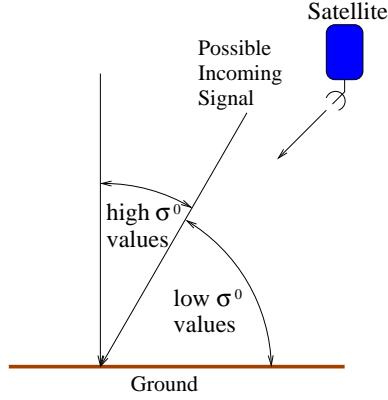


Figure 9: σ^0 dependence on incidence angle for scatterometers.

In the case of the QuikSCAT CGS, for each surface patch in question, θ_{out} is higher than 45° , as seen in Figures 7 and 6. In light of this result, -10 dB for buildings and -20 dB for terrain are reasonable worst case estimates for σ^0 .

Analysis Results and Conclusion

Applying the appropriate parameters and simplifications to Equation (4) yields the interference-to-noise ratios shown in Figure 10.

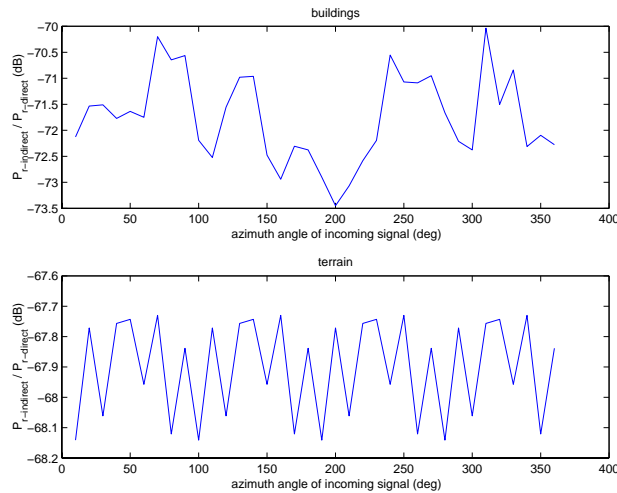


Figure 10: Interference-to-signal ratio as a function of azimuth angle of incoming signal. Depending on the location of the satellite, the azimuth angle of the signal will vary, changing the geometry of the problem. The results, however, show only a minimal dependence on the azimuth angle.

Figure 10 shows that the interference-to-signal ratio of the analyzed multipath is lower than 60 dB for all azimuth angles of the incoming signal. On a linear scale, this means that the interference caused by multipath has less than one millionth the strength of the incoming signal. For the QuikSCAT CGS, this is an acceptable value.

Figure 11 shows a graph of the progressive summation of the interference-to-signal ratio. For the buildings, it continues to increase until all scattering surfaces are summed. For the terrain, the contribution becomes less and less with increasing distance from the CGS. It levels off around -68 dB. This justifies the cutoff at 500m used in this analysis.

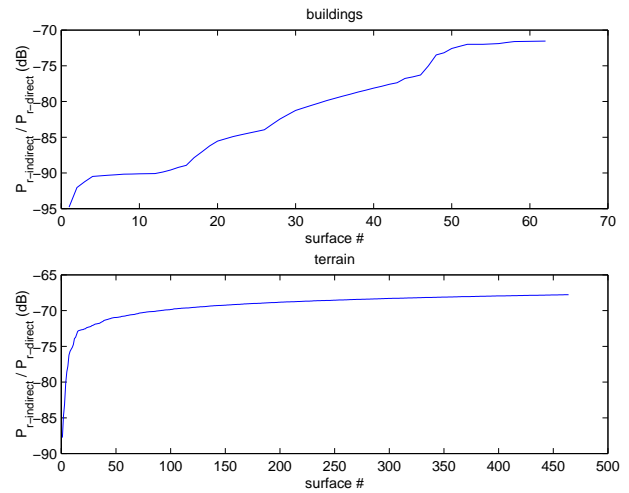


Figure 11: Summation of interference-to-signal ratio. The results level off for the terrain, justifying the 500m cutoff.

The presented analysis shows that multipath off of surrounding buildings and terrain causes negligible effects on the received signal at the CGS. This eliminates the need to compensate for its effects in the ground processing of the CGS data.

REFERENCES

- [1] F. T. Ulaby, R. K. Moore, and A. K. Fung, *Microwave Remote Sensing*, vol. 2. Norwood, MA: Artech House Inc., 1981.
- [2] H. R. Raemer, *Radar Systems Principles*. CRC Press, Inc., 1997.